Available online at www.sciencedirect.com
SCIENCE DIRECT®
Journal of Sound and Vibration 273 (2004) 493–513
JOURNAL OF SOUND AND VIBRATION
www.elsevier.com/locate/jsvi

Bifurcation in an inverted pendulum with tilted high-frequency excitation: analytical and experimental investigations on the symmetry-breaking of the bifurcation

Hiroshi Yabuno[a,*], Makoto Miura[b], Nobuharu Aoshima[a]

[a] *Institute of Engineering Mechanics and Systems, University of Tsukuba, Tsukuba-City 305-8573, Japan*
[b] *Masters Program in Science and Engineering and Systems, University of Tsukuba, Tsukuba-City 305-8573, Japan*

Received 7 May 2002; accepted 28 April 2003

Abstract

In this study, we investigate the dynamics of an inverted pendulum subjected to high-frequency excitation. In particular, we focus on bifurcation phenomena in the dynamics and analyze the effect of the tilt of the excitation direction with respect to gravity direction on the bifurcation. It is analytically clarified that the tilt produces stable equilibrium states different from the directions of the gravity and the excitation. The stability of the stable equilibrium states under the effect of the tilt is discussed non-locally. Also, an analogy of the bifurcation of the inverted pendulum to that of the buckling phenomenon is presented. The theoretically predicted effects of the tilt are qualitatively confirmed by performing some experiments.

1. Introduction

A simple pendulum has an unstable equilibrium state in the upright position. The lateral movement of the pivot by feedback control with respect to the angle and the angular velocity of the pendulum is a well-known method of stabilization of the inverted pendulum, and the stabilization of the inverted pendulum by the feedback control is often treated as a good example of the application of modern control theory (for example [1]). In this study, we focus on another stabilization method with no feedback control which has been recognized in the field of mechanics for a considerably long time [2]. High-frequency excitation in the gravity direction realizes the

*Corresponding author. Tel.: +81-298536473; fax: +81-298535207.
E-mail address: yabuno@esys.tsukuba.ac.jp (H. Yabuno).

0022-460X/03/$ - see front matter
doi:10.1016/S0022-460X(03)00507-8

stabilization of the unstable equilibrium state (upright position), which is the so-called "dynamics stabilization" [3]. In recent years, the effect of the tilt of the excitation direction from the gravity direction on dynamics stabilization has been a focus of research. In the case with a small tilt, the occurrence of many kinds of bifurcations was numerically examined and the non-linear characteristics of the bifurcations were compared with the case of the purely vertical excitation in the gravity direction by Sudor and Bishop [4]. Weibel et al. theoretically analyzed the dynamics of the high-frequency excited pendulum for the case with large tilt using Melnikov theory and Poincaré maps [5]. There have been few experimental approaches taken for dynamics stabilization [6–8], and there is no reported experimental investigation on the effect of the tilt of the excitation direction, to our knowledge.

In this study, we examine the effect of the tilt of the excitation direction analytically and experimentally. In the analytical approach, it is necessary to separate the motion into components depending on a slow time scale and a fast time scale, because the dynamics of the high-frequency excited pendulum is represented as a superposition of fast oscillations and slow evolution. To this end, the method of direct separation of motions [3] and the method of multiple time scales with two time scales have been applied [9,10]. We propose here a more systematic analytical approach by introducing three time scales, which is similar to the method proposed to analyze a non-linear system with high-frequency modulation [11]. This approach is essentially different from the above method of multiple time scales with two time scales, because it is a more straightforward method; introducing more than three time scales makes it possible to yield a higher approximate solution and the procedure of averaging is not needed. Using this method, we transform the equation of motion of the pendulum which is a non-autonomous equation into an autonomous equation. Then the bifurcation equation is derived and the bifurcation analysis is performed. We analytically show the dependence of the inverted position on the variations of the excitation frequency and the excitation amplitude due to the tilt of the excitation direction. The difference between the maximum values of the potential at the two unstable stable equilibrium states, which is produced by symmetry-breaking due to the tilt of the excitation direction, causes a different manner of divergence of the dynamics of the pendulum in the case of a large initial angle so that the pendulum cannot be stabilized in the inverted position. The phenomenon is discussed in relation to the basin boundary of the inverted position and the non-local dependence of the initial angle on the stability. Also, by bifurcation analysis near the bifurcation point, bifurcation of the pendulum analogous to the buckling phenomenon is indicated. Furthermore, through experiments performed with a simple apparatus, theoretically predicted characteristics of the inverted pendulum depending on the tilt of the excitation direction are qualitatively confirmed.

2. Governing equation

The analytical model of an inverted pendulum with a high-frequency excitation is shown in Fig. 1. It consists of a bob of mass m attached to one end of a light rod of length l. The other end is periodically excited along the axis which is tilted in the gravity direction with angle γ. The amplitude and frequency of excitation displacement are a and N. Then the kinetic energy K and

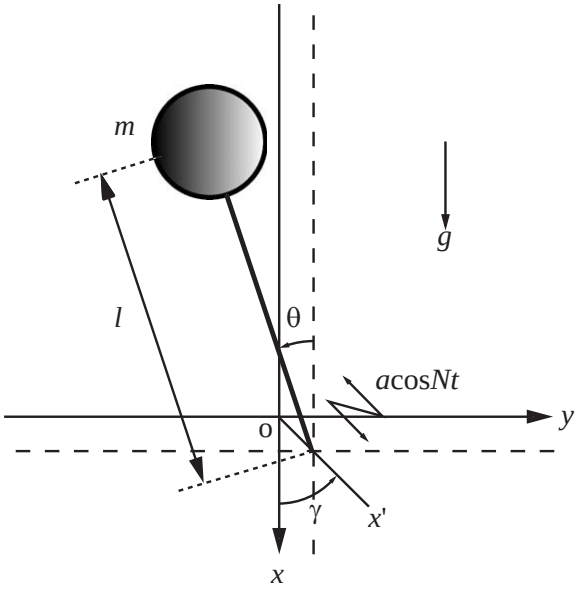

Fig. 1. Analytical model.

potential energy V are expressed as

$$K = \frac{1}{2}m\left\{ l^2\left(\frac{\mathrm{d}\theta}{\mathrm{d}t}\right)^2 + a^2N^2\sin^2 Nt - 2laN\frac{\mathrm{d}\theta}{\mathrm{d}t}(\cos\gamma\sin\theta - \sin\gamma\cos\theta)\sin Nt\right\}, \tag{1}$$

$$V = mgl(\cos\theta - 1). \tag{2}$$

The *Lagrangian* is defined by $L = K - V$ and the *Lagrange's equation of motion* is expressed as

$$\frac{\mathrm{d}}{\mathrm{d}t}\left(\frac{\partial L}{\partial(\mathrm{d}\theta/\mathrm{d}t)}\right) - \frac{\partial L}{\partial\theta} = 0. \tag{3}$$

Then, the equation of motion is obtained:

$$\frac{\mathrm{d}^2\theta}{\mathrm{d}t^2} - \frac{g}{l}\sin\theta - \frac{aN^2}{l}(\cos\gamma\sin\theta - \sin\gamma\cos\theta)\cos Nt = 0. \tag{4}$$

The length and time are normalized using l and $1/N$ respectively. We denote the dimensionless quantities of t and a with t^* $(= Nt)$ and a^* $(= a/l)$. Then, by taking into account a slight viscous damping effect, we obtain the dimensionless equation of motion

$$\ddot{\theta} + \mu\dot{\theta} - \omega^2\sin\theta - a\sin(\theta - \gamma)\cos t = 0, \tag{5}$$

where $\omega^2 = (g/l)/N^2$; ω denotes the ratio of the excitation frequency to the natural frequency of the pendulum around the state, where the pendulum hangs down, in a linear sense. The dot denotes the derivative with respect to t^*. In Eq. (5) and hereafter, the asterisk is omitted.

3. Theoretical analysis

3.1. Bifurcation equation

In this section, we derive an approximate bifurcation equation from the equation of motion. Before applying the analytical method, we perform the scaling of some parameters according to

$$\omega^2 = \varepsilon^2\hat{\omega}^2, \quad a = \varepsilon\hat{a}, \quad \mu = \varepsilon\hat{\mu}, \tag{6}$$

where ^ denotes "of the order $O(1)$" and ε is a bookkeeping device. Then, the dimensionless equation of motion is

$$\ddot{\theta} - \varepsilon^2\hat{\omega}^2 \sin\theta - \varepsilon\hat{a}\sin(\theta-\gamma)\cos t = 0. \tag{7}$$

We analyze Eq. (7) using the method of multiple scales [12] introducing three time scales. We seek an approximate solution in the form

$$\theta(t;\varepsilon) = \theta_0(t_0,t_1,t_2) + \varepsilon\theta_1(t_0,t_1,t_2) + \varepsilon^2\theta_2(t_0,t_1,t_2) + \cdots, \tag{8}$$

where $t_0 = t$, $t_1 = \varepsilon t$, and $t_2 = \varepsilon^2 t$. Substituting Eq. (8) into Eq. (7) and equating coefficients of like powers of ε yield the following equations of the orders $O(1)$, $O(\varepsilon)$, and $O(\varepsilon^2)$:

$$O(1): \quad D_0^2\theta_0 = 0, \tag{9}$$

$$O(\varepsilon): \quad D_0^2\theta_1 = -2D_0D_1\theta_0 - \hat{\mu}D_0\theta_0 + \hat{a}\sin(\theta_0-\gamma)\cos t_0, \tag{10}$$

$$\begin{aligned} O(\varepsilon^2): \quad D_0^2\theta_2 = &-2D_0D_1\theta_1 - 2D_0D_2\theta_0 - D_1^2\theta_0 - \hat{\mu}(D_0\theta_1 + D_1\theta_0) \\ &+ \hat{\omega}^2\sin\theta_0 + \hat{a}\cos(\theta_0-\gamma)\theta_1\cos t_0, \end{aligned} \tag{11}$$

where $D_n = \partial/\partial t_n$. The general solution of Eq. (9) can be written as

$$\theta_0 = c_1(t_1,t_2)t_0 + c_0(t_1,t_2). \tag{12}$$

We note that the first term is a secular term. For a uniform expansion, this term must be eliminated by setting c_1 to zero. Then the general solution becomes

$$\theta_0 = c_0(t_1,t_2). \tag{13}$$

We substitute Eq. (13) into Eq. (10) and obtain

$$D_0^2\theta_1 = \hat{a}\sin(\theta_0-\gamma)\cos t_0. \tag{14}$$

The right-hand side does not contain any terms that produce secular terms in θ_1. The particular solution of Eq. (14) becomes

$$\theta_1 = -\hat{a}\sin(\theta_0-\gamma)\cos t_0. \tag{15}$$

Furthermore, substituting θ_1 into Eq. (11), we have

$$\begin{aligned} D_0^2\theta_2 = &-D_1^2\theta_0 - \hat{\mu}D_1\theta_0 + \hat{\omega}^2\sin\theta_0 - \tfrac{1}{4}\hat{a}^2\sin 2(\theta_0-\gamma) \\ &+ \{2\hat{a}\cos(\theta_0-\gamma)D_1\theta_0 + \hat{\mu}\hat{a}\sin(\theta_0-\gamma)\}\sin t_0 \\ &- \tfrac{1}{4}\hat{a}^2\sin 2(\theta_0-\gamma)\cos 2t_0. \end{aligned} \tag{16}$$

Because the terms which do not contain $\sin t_0$ and $\cos 2t_0$ produce a secular term in θ_2, the sum of these terms must be set to zero as follows:

$$D_1^2\theta_0 + \hat{\mu}D_1\theta_0 - \hat{\omega}^2 \sin\theta_0 + \tfrac{1}{4}\hat{a}^2 \sin 2(\theta_0 - \gamma) = 0. \tag{17}$$

Then, multiplying both sides by ε^2 yields the following equation:

$$\ddot{\theta}_0 + \mu\dot{\theta}_0 - \omega^2 \sin\theta_0 + \tfrac{1}{4}a^2 \sin 2(\theta_0 - \gamma) = 0. \tag{18}$$

Because θ is equal to θ_0 in neglecting the error of $O(\varepsilon)$ from Eq. (8), we can approximately express θ by θ_0. Therefore from Eq. (18), the equation governing the motion of the pendulum can be described as follows:

$$\ddot{\theta} + \mu\dot{\theta} - \omega^2 \sin\theta + \tfrac{1}{4}a^2 \sin 2(\theta - \gamma) = 0. \tag{19}$$

As a result, the governing equation (5), which is non-autonomous, is transformed into the autonomous differential equation (19) by using the method of multiple scales with three time scales. Also, Eq. (19) with $\mathrm{d}^2/\mathrm{d}t^2 = \mathrm{d}/\mathrm{d}t = 0$ leads to the bifurcation equation

$$F \equiv \omega^2 \sin\theta - \tfrac{1}{4}a^2 \sin 2(\theta - \gamma) = 0. \tag{20}$$

3.2. Higher order analysis in the steady state

In this section we discuss the small oscillation which is mentioned in Refs. [13,14]. The solution of the order of $O(\varepsilon)$ is expressed from Eqs. (8) and (15) as follows:

$$\varepsilon\theta_1 = -\varepsilon\hat{a} \sin(\theta_0 - \gamma)\cos t_0 = a \sin(\theta_0 - \gamma)\cos t_0 \approx a(\theta_0 - \gamma)\cos t_0. \tag{21}$$

Also, from Eq. (18) with $\ddot{\theta}_0 = \dot{\theta}_0 = 0$, θ_0 in the steady state satisfies the following equation:

$$\theta_0 = \frac{a^2\gamma}{a^2 - 2\omega^2}, \tag{22}$$

where $O(\theta^2)$ is neglected. Substituting Eq. (22) into Eq. (21), we can rewrite $\varepsilon\theta_1$ as follows:

$$\varepsilon\theta_1 = \frac{2a\omega^2\gamma}{a^2 - 2\omega^2}\cos t_0 \approx \frac{2\omega^2\gamma}{a}\cos t_0, \tag{23}$$

where we assume $\omega^2/a^2 \ll 1$. Therefore, the small oscillation has the same frequency as the excitation frequency and the amplitude is in inverse proportion to the excitation amplitude.

3.3. Bifurcation analysis

Equilibrium states satisfy the bifurcation equation (20). Their stabilities can be also estimated by using the potential energy of the system. The equivalent dimensionless potential energy U is expressed using F as follows:

$$U = -\int F\,\mathrm{d}\theta = \omega^2 \cos\theta - \tfrac{1}{8}a^2 \cos 2(\theta - \gamma). \tag{24}$$

We can estimate the stability of the equilibrium states by the sign of $\mathrm{d}^2U/\mathrm{d}\theta^2$ $(= \mathrm{d}F/\mathrm{d}\theta)$ according to the argument in Ref. [15].

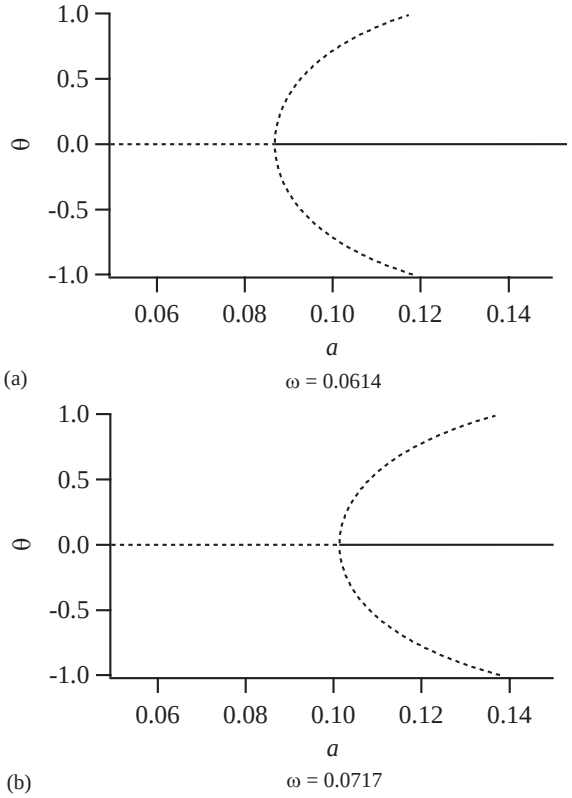

Fig. 2. Bifurcation diagram of a vs. θ ($\gamma = 0$).

3.3.1. Variation of the stable inverted states depending on the excitation amplitude

Figs. 2 and 3 show the relationship between the excitation amplitude and the stable inverted states in the cases of vertical excitation along the gravity direction and tilted excitation respectively, where the solid and dashed lines denote stable and unstable equilibrium states respectively. First, from comparing (a) and (b) in Figs. 2 and 3, it is seen that stable equilibrium states exist in a lower excitation amplitude range when the excitation frequency is higher. In the case of the excitation along the gravity direction (along the purely vertical direction), the stable equilibrium states are in the vertical upright position, $\theta = 0$, as shown in Fig. 2 and are independent of the magnitude of the excitation amplitude. On the other hand, when the excitation direction is tilted from the gravity direction, the stable equilibrium states depend on the excitation amplitude and as the excitation amplitude becomes larger, the stable equilibrium states approach excitation direction ($\theta = \gamma$). With decreasing excitation amplitude, the angle of the pendulum θ in the stable equilibrium state becomes more greater than the excitation direction.

3.3.2. Variation of the stable inverted states depending on the excitation frequency

First, we consider the case of purely vertical excitation, i.e., $\gamma = 0$. The upright position ($\theta = 0$) is a possible configuration as seen from Eq. (20). The bifurcation diagram corresponding to the subsequent experiment ($a = 0.09$) is shown in Fig. 4(a), where the stability of the equilibrium state

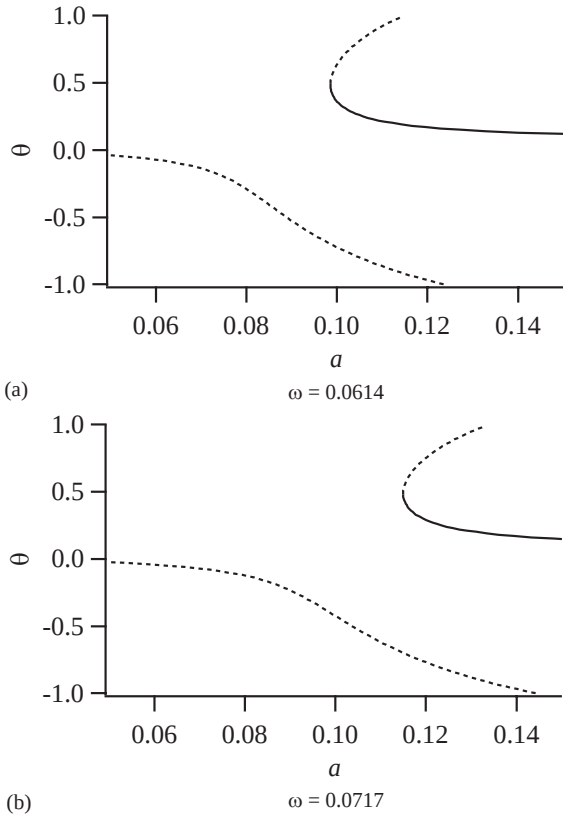

Fig. 3. Bifurcation diagram of a vs. θ ($\gamma = 0.08$).

is examined by the above-mentioned method [15] and the solid and dashed lines denote stable and unstable equilibrium states respectively. The bifurcation at point PF ($\omega = \omega_{cr} = a/\sqrt{2} = 0.005/0.0537 = 0.093$) is symmetric, which is classified as pitchfork bifurcation from the local analysis in Section 3.2.3. If a lower excitation frequency ($\omega > \omega_{cr}$) is applied, the upright position is unstable, i.e., the stable inverted position cannot be realized. However, when the excitation frequency is sufficiently high ($\omega < \omega_{cr}$), it becomes stable.

In the cases of before-bifurcation ($\omega > \omega_{cr}$) and post-bifurcation ($\omega < \omega_{cr}$), the schematic potential curves are described from Eq. (24) as shown in Figs. 5(a) and (b) respectively. The maximum and minimum points of the potential curves correspond to the unstable and stable equilibrium states respectively. Fig. 5(b) shows that the upright position ($\theta = \theta_s = 0$) in the case of $\omega < \omega_{cr}$ is stable. In the case without initial angular velocity, the initial angles between the unstable equilibrium states ($\theta = \theta_{u1}$ and $\theta = \theta_{u2}$) for each excitation frequency realize the upright position of the pendulum after the transient state.

Next, in Fig. 4(b), we show the bifurcation diagram in the case when a slight tilt is applied to the line of the excitation for the gravity direction, i.e., $\gamma \neq 0$. The system undergoes a bifurcation at the point SN; we set ω_{cr} as the value of ω at the point SN. There is a symmetry-breaking imperfection and the upright position ($\theta = 0$) is no longer admissible. In the case when ω is smaller than ω_{cr} and ω is close to ω_{cr}, the stable inverted state (stable equilibrium state) is more inclined than the

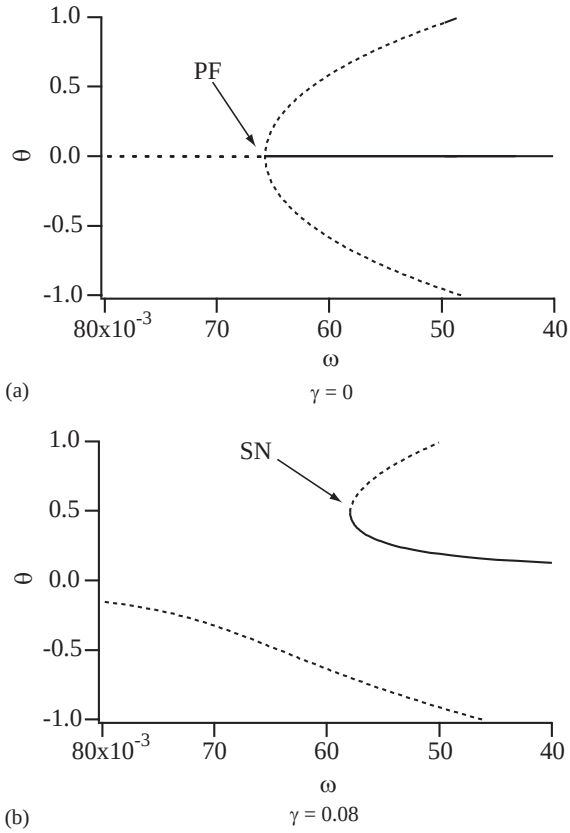

Fig. 4. Bifurcation diagram of ω vs. θ.

tilt of the line of the excitation ($\theta = \gamma$). Henceforth "inverted state" means that the pendulum is stabilized with the angle in the range of $|\theta| < \pi/2$. With increasing excitation frequency, the inclination of the stable inverted state from the excitation direction is decreased and at the limitation of the excitation ($\omega \to 0$), the stable inverted position approaches the excitation direction ($\theta = \gamma$). Now let us examine the global stability of the pendulum for the case of $\gamma > 0$ (the stability in the case of $\gamma < 0$ is contrary to the following results) using the potential curve. In the case of $\omega < \omega_{cr}$, the potential curve is depicted in Fig. 5(c). The two maximum potential energies at θ_{u1} and θ_{u2} are different. The potential energy at the lower unstable equilibrium state ($\theta = \theta_{u1}$) in Fig. 4 is greater than the potential energy at the upper unstable equilibrium state ($\theta = \theta_{u2}$) bifurcated from the saddle-node bifurcation in Fig. 4(b). Therefore, in contrast to the case of purely vertical excitation ($\gamma = 0$), even if the initial angle is between lower and upper unstable equilibrium states for each ω ($< \omega_{cr}$), the pendulum cannot always realize the stable inverted states in the case when the initial angle is near the lower unstable equilibrium state ($\theta = \theta_{u1}$), because sufficient velocity to go beyond the maximum point of the potential curve corresponding to the upper unstable equilibrium state ($\theta = \theta_{u2}$) remains at the upper unstable equilibrium state.

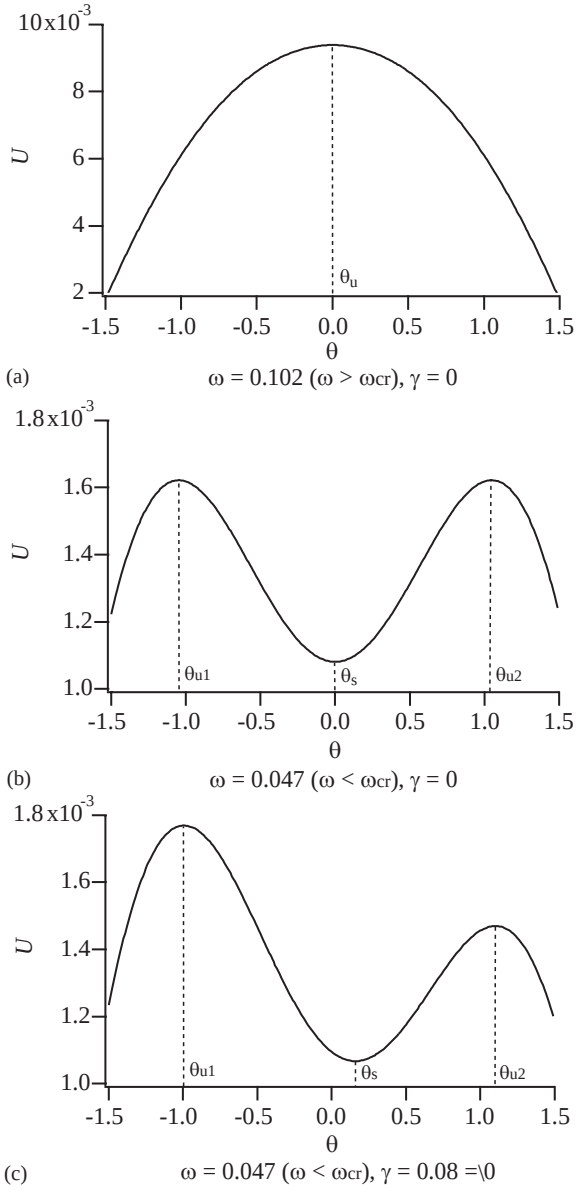

Fig. 5. Potential curves ($a = 0.093$).

3.3.3. *Local bifurcation analysis*

Next, by locally examining the bifurcation, we show that the dynamics of the inverted pendulum is analogous to the buckling phenomenon. Assuming that θ and γ are small, we employ the truncated Taylor series as follows:

$$\sin\theta = \theta - \tfrac{1}{6}\theta^3 + O(\theta^5), \quad \cos\theta = 1 - \tfrac{1}{2}\theta^2 + O(\theta^4),$$
$$\sin\gamma = \gamma, \quad \cos\gamma = 1. \tag{25}$$

Then Eq. (19) is rewritten as

$$\ddot{\theta} + \mu\dot{\theta} + \left(\frac{a^2}{2} - \omega^2\right)\theta + \left(\frac{\omega^2}{6} - \frac{a^2}{3}\right)\theta^3 - \frac{a^2\gamma}{2} = 0. \tag{26}$$

The difference between ω and the critical value for the pitchfork bifurcation mentioned in Section 3.2.2, $\omega_{cr} = a/\sqrt{2}$, is assumed to be very small such as $O(\varepsilon^2)$, where ε is a bookkeeping device different from that in Eq. (6). Then by taking into account $O(\varepsilon^3)$, Eq. (26) is rewritten as

$$\ddot{\theta} + \mu\dot{\theta} + \left(\frac{a^2}{2} - \omega^2\right)\theta - \frac{a^2}{4}\theta^3 - \frac{a^2\gamma}{2} = 0. \tag{27}$$

The above equation has the same form as the equation of motion expressing the buckling phenomenon in the two-link model subjected to compressive force [16] and as the modal equation expressing the well-known classical Euler buckling in a simply supported beam [17]; θ and ω correspond to the displacement of the link or the mid-beam deflection and the compressive force in those models respectively. With $d^2\theta/dt^2 = d\theta/dt = 0$ in Eq. (27), we obtain the bifurcation equation as follows:

$$\left(\frac{a^2}{2} - \omega^2\right)\theta - \frac{a^2}{4}\theta^3 - \frac{a^2\gamma}{2} = 0. \tag{28}$$

This equation is the same as the normal form of pitchfork bifurcation. The bifurcation diagram expressing the relationship between the equilibrium state of the angle θ and ω is easily described from Eq. (27) as shown in Fig. 6. In the case of $\gamma = 0$, the complete pitchfork bifurcation occurs. In the case of $\gamma \neq 0$, symmetry-breaking is produced in the pitchfork bifurcation. Therefore, the last term with γ on the left-hand side in Eq. (27), which is the effect of the tilt of the excitation direction to the gravity direction, corresponds to the effect of the imperfection due to an initial deflection and a gravity force in the above two-link system or a simply supported beam subjected to compressive force [15,18].

Next, we compare the non-linear characteristics of the pitchfork bifurcations which are produced in the buckling problem under the compressive force and in the dynamics of the inverted pendulum with high-frequency excitation. Because the coefficient of θ^3 in Eq. (28) is negative and

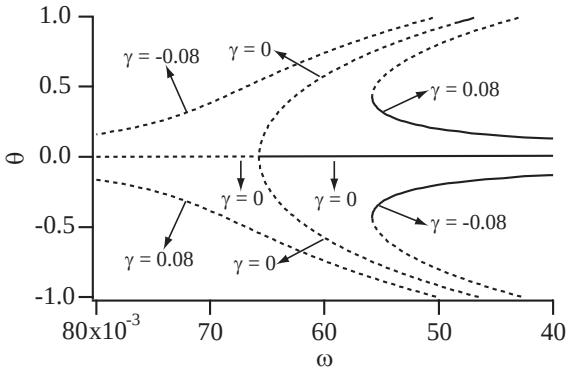

Fig. 6. Approximated bifurcation diagram of ω vs. θ.

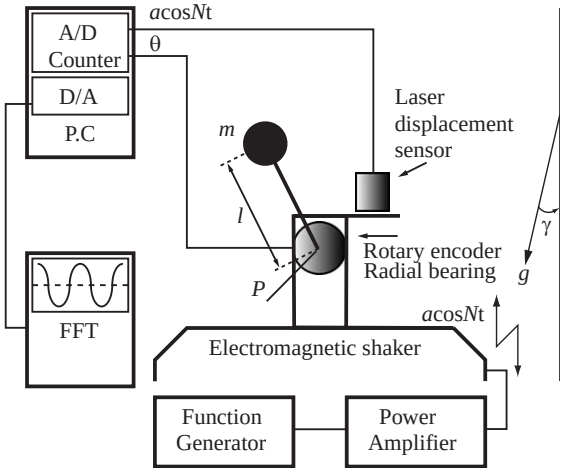

Fig. 7. Experimental apparatus.

the non-linear restoring force is of the soft spring type, the non-linear characteristic of pitchfork bifurcation in the inverted pendulum is subcritical. On the other hand, the non-linear characteristic of the pitchfork bifurcation in the buckling problem under the compressive force is supercritical, as is widely recognized [16,17], because the non-linear restoring force is of the hard spring type. Therefore the non-linear characteristic of the pitchfork bifurcation in the inverted pendulum with high-frequency excitation is not in agreement with that in the buckling problem subjected to the compressive force. However, there is a buckling phenomenon with the same non-linear characteristic as in the case of the inverted pendulum with high-frequency excitation. It is the electromagnetic buckling phenomenon. In this phenomenon, the two-ink system and the simply supported beam subjected to electromagnetic force can undergo subcritical pitchfork bifurcation because the equivalent non-linear restoring force due to the combination of elastic and electromagnetic forces is of the soft spring type [19,20].

4. Experiment

We experimentally investigate the effect of the tilt of the excitation direction γ on the dynamics of the inverted pendulum with high-frequency excitation. In Fig. 7, we show the experimental apparatus. The pendulum is free to swing on the plane with a radial bearing (pivot P) (Fig. 8). The pivot is subjected to high-frequency excitation along a straight line offset by the angle γ from the gravity direction by an electromagnetic shaker. The displacement of the pivot is measured by a laser displacement sensor (KEYENCE Corp., LB-02). The angle of the pendulum is measured by an encoder (Nikon Corp., RXB1000). The bob of mass m and the length of the light rod l of the pendulum are 2.35×10^{-2} kg and 5.37×10^{-2} m respectively. The angle of tilt of the excitation direction γ is calculated using the experimentally measured natural frequency of another pendulum, which is located freely to move on the plane $z - x'$ as shown in Fig. 9.

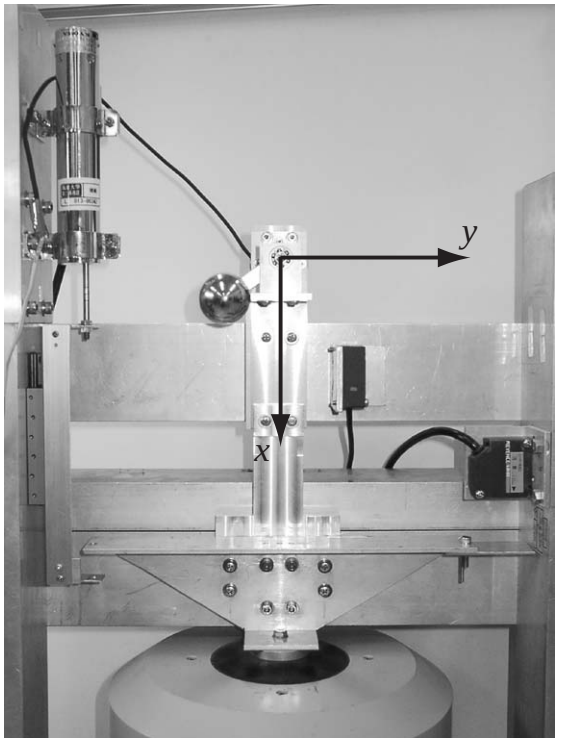

Fig. 8. Photograph of experimental apparatus (in the state of $\gamma = 0$).

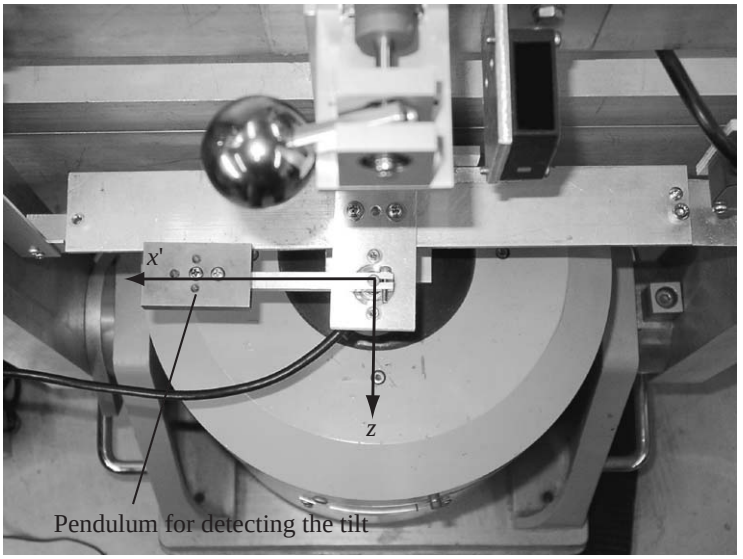

Fig. 9. Measurement of the tilt of the excitation direction.

4.1. Stable inverted states

4.1.1. Variation of the stable inverted states depending on the excitation amplitude

Figs. 10 and 11 show the experimental relationship between the excitation amplitude and the stable equilibrium state in the cases of the vertical excitation approximately along the gravity direction (along the purely vertical direction) and the tilted excitation respectively. The black circle denotes the magnitude of the DC component in the steady state obtained from the spectral analysis, i.e., the stable equilibrium states of the pendulum (these plots correspond to the points on the solid line in Fig. 2); another frequency component theoretically discussed in Section 3.2 is mentioned in the appendix. First, by comparing (a) and (b) in Figs. 10 and 11, it is experimentally demonstrated that the stable equilibrium states exist in a lower excitation amplitude range when the excitation frequency is higher. Next, we can observe the effect of the tilt of the excitation on the stable equilibrium states as theoretically predicted in Fig. 3. In the case of the excitation approximately along the gravity direction (the purely vertical direction), it is noted from Fig. 10 that the stable equilibrium states are close to the vertical upright position, $\theta = 0$, and are only slightly dependent on the magnitude of the excitation amplitude; they are not completely independent because the experimentally observed stable equilibrium states are not purely vertical

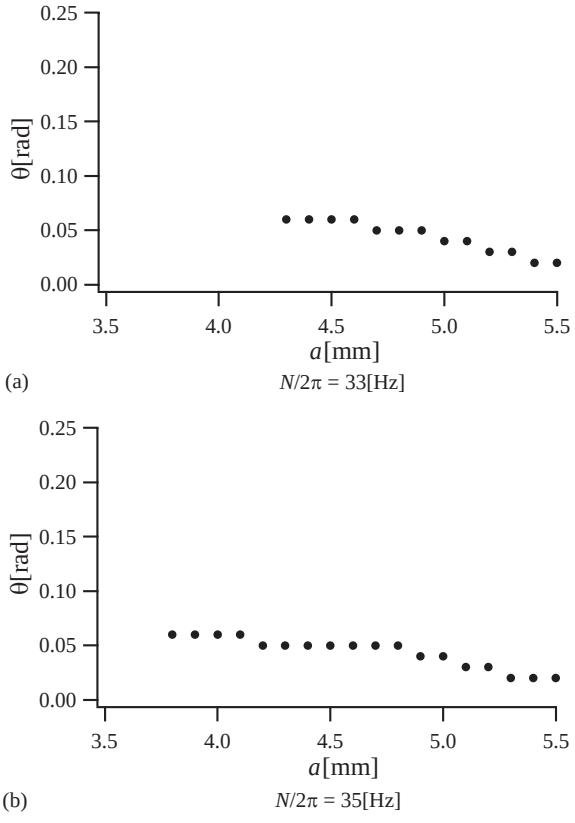

Fig. 10. Bifurcation diagram of a vs. θ ($\gamma = 0$).

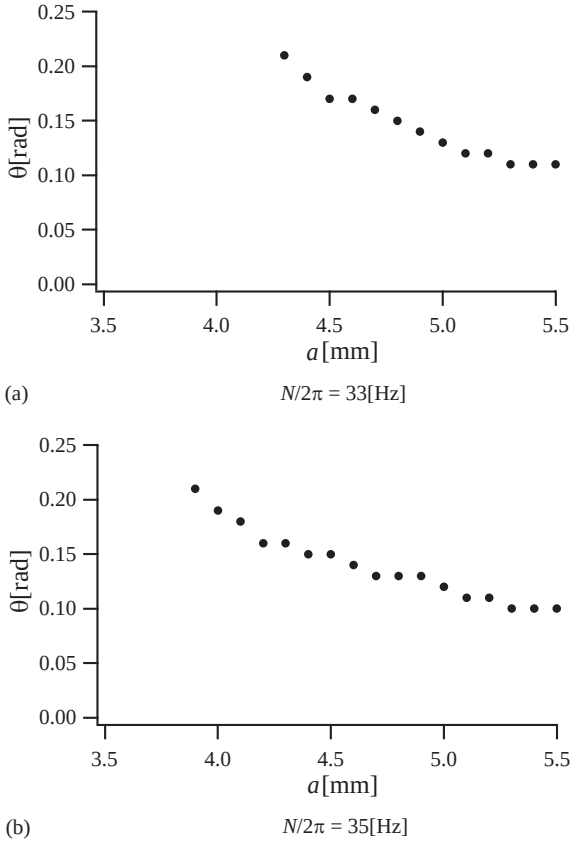

Fig. 11. Bifurcation diagram of a vs. θ ($\gamma = 0.08$).

due to a slight immeasurable tilt of the excitation direction. On the other hand, when the excitation direction is tilted away from the gravity direction, it is noted from Fig. 11 that the stable equilibrium states depend on the excitation amplitude, and as the excitation amplitude becomes larger, the stable equilibrium state approaches the excitation direction ($\theta = \gamma = 0.08$). At a lower excitation amplitude, the angle of the pendulum θ in the stable equilibrium state deviates from the excitation direction ($\theta = \gamma$) and is more inclined, as theoretically shown in Fig. 3.

4.1.2. Variation of the stable inverted states depending on the excitation frequency

Figs. 12(a) and (b) show the experimental relationship between the excitation frequency and the stable equilibrium state in the cases of vertical excitation along the gravity direction and tilted excitation respectively. The black circles denote the magnitude of the DC component in the steady state from the spectral analysis, i.e., the stable equilibrium state of the pendulum (these plots correspond to the points on the solid line in Fig. 4). We cannot observe any stable equilibrium states except in the state, where the pendulum hangs down, in the case when the excitation frequency is lower than $N/2\pi = 31$ Hz. Comparing Figs. 12(a) and (b), we can observe the effect of the tilt of the excitation on the stable equilibrium states as theoretically predicted in Fig. 4. In the case of the excitation approximately along the gravity direction (along the purely vertical

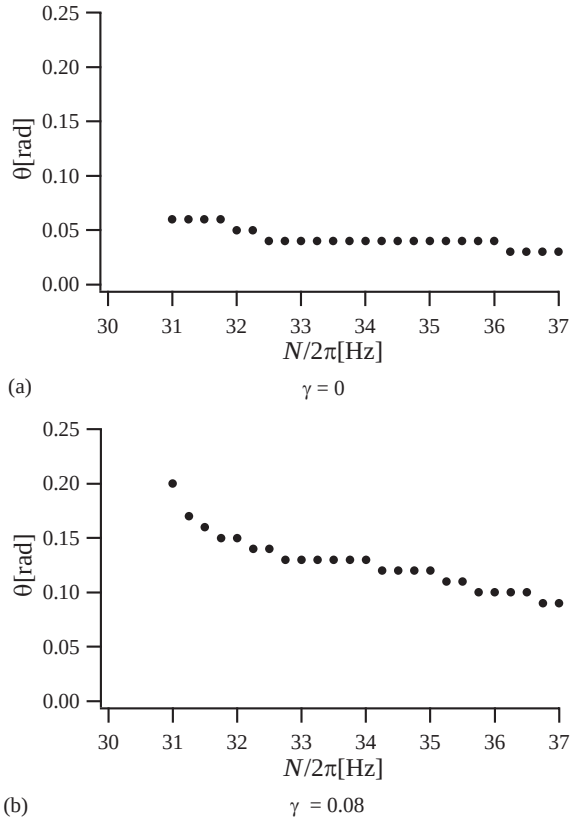

Fig. 12. Bifurcation diagram of ω vs. θ.

direction), it is noted from Fig. 12(a) that the stable equilibrium states are close to the vertical upright position, $\theta = 0$ (the experimentally observed stable equilibrium states are not purely vertical due to a slight immeasurable tilt of the excitation direction), and are only slightly dependent on the magnitude of the excitation frequency. Those stable equilibrium states correspond to the stable equilibrium states in the symmetric subcritical pitch-fork bifurcation (the bifurcation is not perturbed because the excitation direction is not tilted), as theoretically shown in Fig. 4(a). On the other hand, when the excitation direction is tilted away from the gravity direction, it is noted from Fig. 12(b) that the stable equilibrium state depends on the excitation frequency and as the excitation frequency becomes larger, the stable equilibrium state approaches the excitation direction ($\theta = \gamma = 0.008$). At a lower excitation frequency, the angle of the pendulum θ in the stable equilibrium state deviates from the excitation direction ($\theta = \gamma$) and is more inclined, as theoretically shown in Fig. 4(b).

4.2. Experimental basin for the stable inverted states

We experimentally examine the dependence of the initial angle on the possibility of the accomplishment of the inverted position in the case of tilted excitation. We set various excitation frequencies and set the initial angles at white circles, white triangles, and at other locations

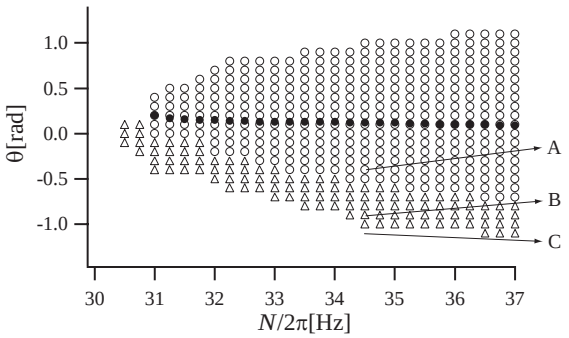

Fig. 13. Global stability of the upright position.

without any initial angular velocity in Fig. 13. In the case when the initial angle is $\theta(0) = -0.37$ rad (point A in Fig. 13) and the excitation frequency and amplitude are $N/2\pi = 34.5$ Hz and $a = 0.005$ m, respectively the time history converges to stable equilibrium state close to the upright position. As well as this case, all time histories in the cases with the initial angles marked with the white circles in Fig. 13 converge to stable equilibrium states close to the upright position marked with the black circles for each excitation frequency. On the other hand, in the case when the initial angle is $\theta(0) = -1.081$ (point C in Fig. 13) (this condition is included in the region without marks), the time history deviates from the upright position to the state, where the pendulum hangs down, with time as seen in Fig. 14(c). At all initial angles in the region without marks, a qualitatively similar time history is observed.

In the case when the initial angle is positive ($\theta(0) = -0.93$ at point B in Fig. 13), another transient state is observed. Hence the pendulum passes the upright position and then travels to the state, where the pendulum hangs down, through the state with an angle with a positive sign which is opposite to the sign of the initial angle $\theta(0) < 0$. A similar transient state is observed in the case of the initial angle denoted by triangles $\triangle$ in Fig. 13. This phenomenon experimentally shows that the maximum value of the potential at the lower unstable equilibrium state ($\theta = \theta_{u1}$ in Fig. 5) of the bifurcation diagram is higher than that of the potential at the upper unstable equilibrium state ($\theta = \theta_{u2}$ in Fig. 5) bifurcated from the saddle-node bifurcation, as theoretically discussed in Section 3.2.3.

5. Conclusions

This work addresses the inverted dynamics of a high-frequency-excited pendulum. The non-autonomous equation of motion is transformed into an autonomous equation using the method of multiple time scales introducing three time scales. Because this approach is systematic, the derivation of a higher order approximate solution can be derived in a straightforward manner by introducing more time scales. From bifurcation analysis using the obtained autonomous equation, it is analytically shown that symmetry-breaking due to the effect of the tilt of the excitation direction produces stable equilibrium states (inverted states) which are in a different direction from the excitation direction and the gravity direction. The angle of inclination of the pendulum in the stable equilibrium state is much greater than the excitation direction, and with

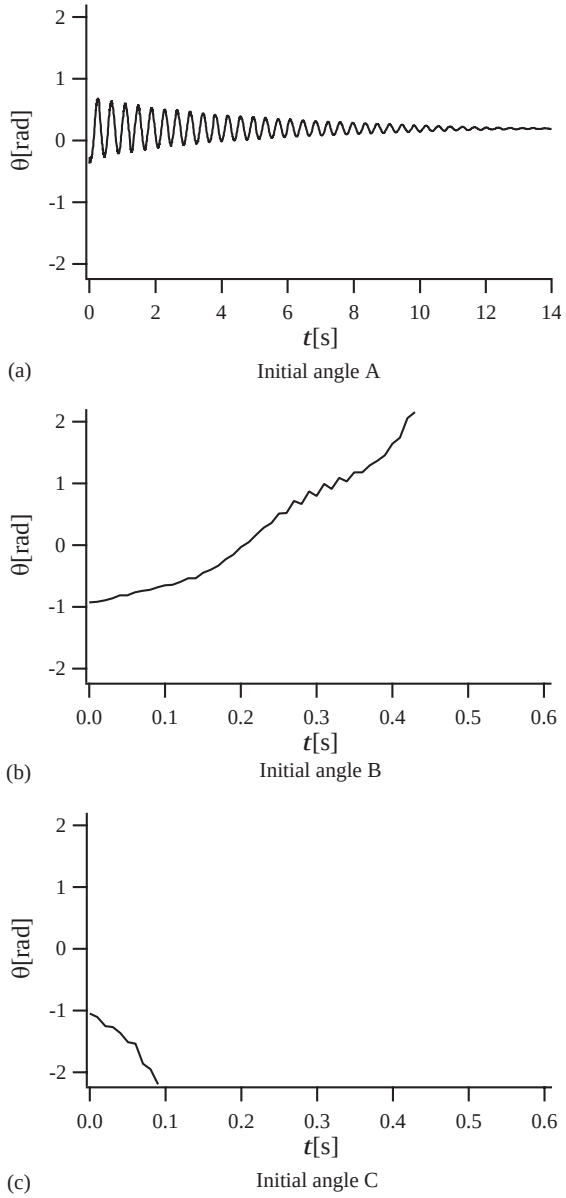

Fig. 14. Transient responses.

increasing excitation frequency, the angle approaches the excitation direction. The basin boundary for the realization of the inverted position is expressed by the region between two unstable equilibrium states which are not bifurcated and produced through saddle-node bifurcation. It is noted that the potential energy at the former unstable equilibrium state is higher than the potential energy at the latter one. Also, the analogy of the local dynamics of the pendulum to the buckling phenomenon is presented and it is clarified that the excitation frequency

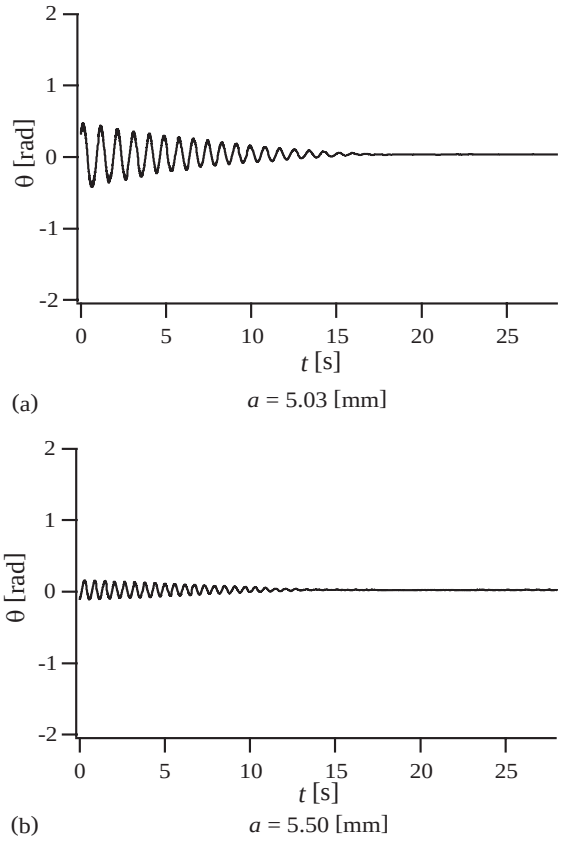

Fig. 15. Time histories of the pendulum.

and the tilt of the excitation correspond to the effects of the compressive force and transverse force in Euler-buckling under compressive force respectively. Furthermore, experiments using a simple apparatus are performed. Experimentally obtained bifurcation diagrams are in qualitative agreement with theoretical ones. It is experimentally observed that the inverted positions are more inclined than the excitation direction by symmetry-breaking of the bifurcation due to the tilt of the excitation direction. From the comparison among the transient responses for some initial angles, the difference between the potential energy at two unstable equilibrium states is experimentally confirmed.

Acknowledgements

The first author wishes to thank Professor J.J. Thomsen (Department of Solid Mechanics, Technical University of Denmark) who gave a very impressive presentation on interesting phenomena under high-frequency excitation at ICTAM 2000 and a detailed list of papers on

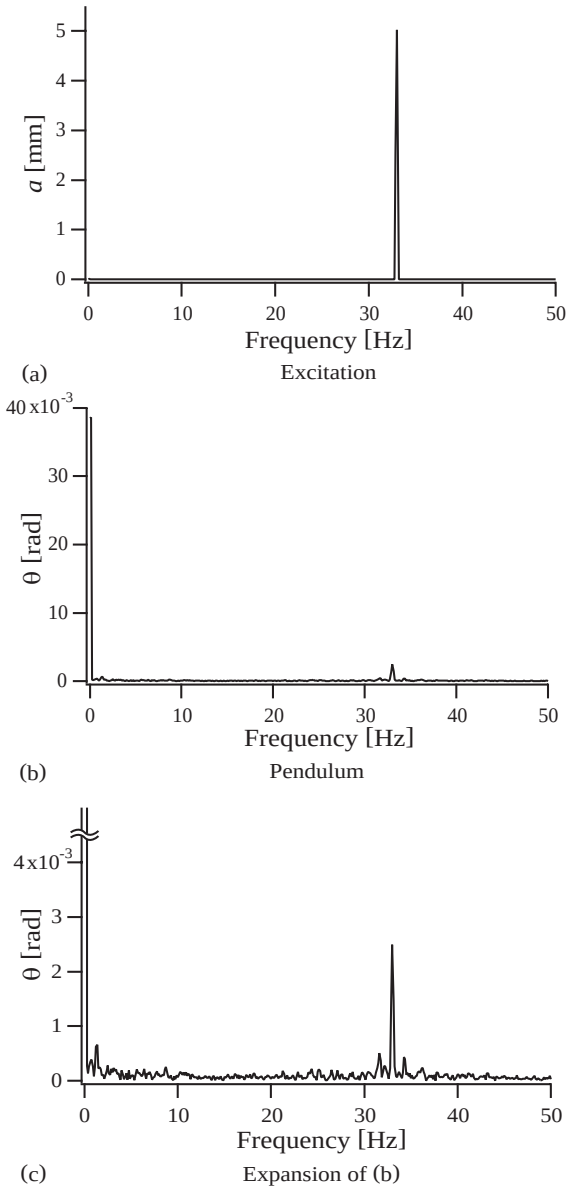

Fig. 16. Frequency components in the steady state ($a = 5.03$ mm).

dynamics under high-frequency excitation. All authors express their thanks to Mr. R. Kanda and Mr. T. Murakami, graduate students of University of Tsukuba for their assistance. Interesting comments by one of the reviewers are gratefully acknowledged. This work was supported by Grants-in-Aid for Scientific Research of Japanese Ministry of Education, Culture, Sports, Science and Technology Nos. 13650243 and 09650454.

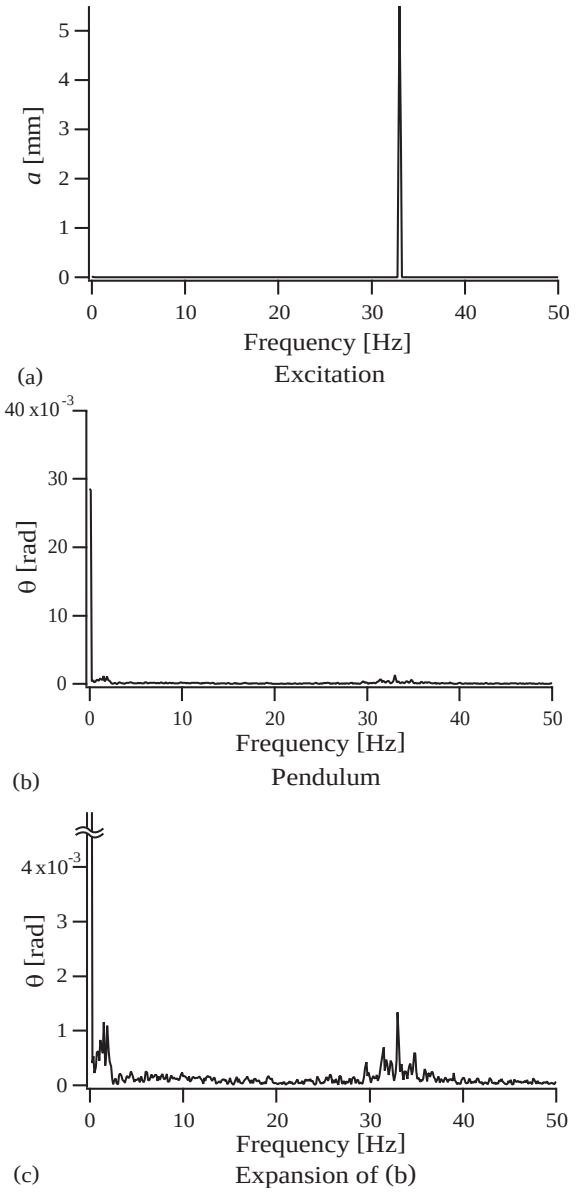

Fig. 17. Frequency components in the steady state ($a = 5.50$ mm).

Appendix

Fig. 15 shows the time histories including the transient state in the cases of the excitation amplitude, $a = 5.03$ and 5.50 mm. As theoretically indicated in Section 3.2, it is experimentally confirmed from their power spectra in the steady state, Figs. 16 and 17, that the steady states of the pendulum include the excitation frequency component and the magnitude is increased as the excitation amplitude decreases.

References

[1] K. Ogata, *Modern Control Engineering*, Prentice-Hall, Englewood Cliffs, NJ, 1970.
[2] A. Stephenson, On a new type of dynamical stability, *Memoirs and Proceedings of the Manchester Literary and Philosophical Society* 52 (1908) 1–10.
[3] P.L. Kapitza, in: D. Ter Haar (Ed.), *Collected Papers by P.L. Kapitza*, Vol. 2, Pergamon Press, London, 1965, pp. 714–726.
[4] D.J. Sudor, S.R. Bishop, Inverted dynamics of a tilted parametric pendulum, *European Journal of Mechanics A/Solids* 18 (1996) 517–526.
[5] S. Weibel, J. Taper, U. Baillieul, Global dynamics of a rapidly forced cart and pendulum, *Nonlinear Dynamics* 13 (1997) 131–170.
[6] M.M. Michaelis, Stroboscopic study of the inverted pendulum, *American Journal of Physics* 53 (1985) 1079–1083.
[7] H.P. Kalmus, The inverted pendulum, *American Journal of Physics* 38 (1970) 874–878.
[8] H.J.T. Smith, K.A. Blackburn, Experimental study of an inverted pendulum, *American Journal of Physics* 60 (1992) 909–911.
[9] A. Fildlin, On the separation of motions in systems with a large fast excitation of general form, *European Journal of Mechanics A/Solids* 18 (1999) 527–538.
[10] J.S. Jensen, Buckling of an elastic beam with added high-frequency excitation, *International Journal of Non-Linear Mechanics* 35 (2000) 217–227.
[11] S.A. Nayfeh, A.H. Nayfeh, The response of nonlinear systems to modulated high-frequency input, *Nonlinear Dynamics* 7 (1995) 301–315.
[12] A.H. Nayfeh, D.T. Mook, *Nonlinear Dynamics*, Wiley, New York, 1979.
[13] M.J. Clifford, S.R. Bishop, Inverted oscillations of a driven pendulum, *Proceedings of the Royal Society of London A* 454 (1998) 281–2817.
[14] S.R. Bishop, D.J. Sudor, The 'not quite' inverted pendulum, *International Journal of Bifurcation and Chaos* 9 (1999) 273–285.
[15] M. Golubitsky, D.G. Schaeffer, *Singularities and Groups in Bifurcation Theory*, Springer, New York, 1985.
[16] J.J. Stoker, *Nonlinear Vibrations in Mechanical and Electrical Systems*, Wiley, New York, 1950.
[17] S.P. Timoshenko, J.M. Gere, *Theory of Elastic Stability*, McGraw-Hill, New York, 1961.
[18] J.M.T. Thompson, G.W. Hunt, *Elastic Instability Phenomena*, Wiley, Chichester, 1984.
[19] H. Yabuno, M. Yoshizawa, Postbuckling behavior and nonlinear parametrically-excited oscillation of the current carrying-beam (analysis by using computer algebra), Proceedings of the Japan-CIS Joint Seminar on Electro Magneto Mechanics, Tokyo, 1992, pp. 93–96.
[20] H. Yabuno, Y. Kurata, N. Aoshima, Effect of coulomb damping on buckling of a two-rod system, *Nonlinear Dynamics* 15 (1998) 207–224.